

# Investigation of solders surface tension in temperature range from melting point up to 673K

Plamen V. Petkov<sup>\*1</sup> Dimitar Lyutov<sup>2</sup>, and Hristo Iliev<sup>3</sup>  
 pvpetkov@phys.uni-sofia.bg<sup>\*1</sup> d\_lyutov@phys.uni-sofia.bg<sup>2</sup> h\_iliev@phys.uni-sofia.bg<sup>3</sup>  
 Sofia University St Kliment Ohridski, 5 James Bourchier Blvd. 1164 Sofia, Bulgaria

**Abstract** Solders are fusible metal alloys, used in industry to create permanent bond between metal surfaces. In order to achieve this, solders need to be heated above their melting point and used in liquid phase. Low melting temperature is essential from technological point of view, as well as for soldered components safety. Typical solders have Lead (Pb) as a base component, having melting temperature of 600.6 K. Adding up to 60% of Tin (Sn) to the alloy, reduces melting temperature down to 456-461 K in average. Since 2006, RoHS regulation enforce industrial use of Lead-Free solders, typically having much higher melting temperature. However, Pb:Sn solders with up to 40% Sn still have their industrial applications, usually used for soldering Cu and Zn coated pipes while the 60% Sn containing solders are used for soldering of electrical cables.

The achieving of these goals requires knowledge of liquid phase surface tension. Because of the difficulties, related to such measurement, the available data in literature are limited. The current report presents an equipment for measurement of the surface tension, based on the Wilhelmy plate method as well as the applied measurement procedure. The Wilhelmy method has relatively good stability. The contact angle also can be considered zero for the examined samples therefore correction coefficients are not required for the measurement. The results from measurement of Pb:Sn in ratio 40:60 and also in ratio 60:40 show that the oxidation in excess of Pb lowers the surface tension while for the case with excess of Sn, the oxidation lead to increase of the surface tension if compare with the surface tension obtained for the same solders but under non-oxidizing conditions. This could be attributed to formation in excess of PbO and SnO on the liquid surface of the corresponding solder.

**Keywords:** TIN, LEAD, SOLDER, SURFACE TENSION, NUCLEAR REACTOR, OXIDIZING

## 1. Introduction

Solders are fusible metal alloys, used in industry to create permanent bond between metal surfaces. In order to achieve this, solders need to be heated above their melting point and used in liquid phase. Low melting temperature is essential from technological point of view, as well as for soldered components safety, because this way is achieved significant temperature difference from the critical temperature of the soldered components

Reports for the surface tension of liquid Pb:Sn mixture exists for more than a century, since the beginning of their application as a solder. The work by Bircumshaw, [1], Whites [2] and Kucharski et al., [3] provide detailed study on the surface tensions. The studies were further extended on wettability, by Gasior et al [4]. A summary of the available data as well as their independent verification is provided in [5, 6] under non-oxidation conditions. The phase diagram of Pb:Sn system is established for long time [7], but because of the importance of the topic, the studies on solidification and liquation still continue and the newer studies are ongoing, [8, 9] Obviously the accurate knowledge of phase diagram represents importance for surface tension measurement.

Typical solders have Lead (Pb) as a base component, having melting temperature of 600.6 K. Adding up to 60% of Tin (Sn) to the alloy, reduces melting temperature down to 456-461 K in average. Since 2006, RoHS regulation enforce industrial use of Lead-free solders, typically having much higher melting temperature. However, Pb:Sn solders with up to 40% Sn still have their industrial applications, usually used for soldering Cu and Zn coated pipes while the 60% Sn containing solders are used for soldering of electrical cables.

More recent application of Pb contained liquid alloys became important with the development of nuclear technology. The most popular of these alloys is Pb:Bi eutectic mixture because of the low melting temperature [10]. However, the potential of Pb:Sn alloys is known and they are currently under consideration [11].

## 2. Theoretical background

Surface tension of liquid soldering alloys plays important role in the process of soldering. It also has significant impact on the thermal properties of the soldering process, including the cooling stability. The lower surface tension facilitates the soldering process

and improves the property, called solderability. The appropriate surface tension ranges within 400-700 mN/m, [12]. In different proportion of their constituents, these alloys have found significant applications in the industry and the determination of their surface tension is important and challenging task. Thus, our interest is focused on investigation of the binary Pb:Sn alloys, used in low temperature soldering process.

Recent studies, reported in Ref. [5], provided an empirical correlation between the constituent proportions, that allows us to calculate the surface tension:

$$\sigma_{i,j} = \sigma_{Pb}X_{Pb} + \sigma_{Sn}X_{Sn} + (826.8 - 0.5526T)X_{Pb}^2 + (-420.4 + 0.3270T)X_{Pb}^3 \quad (1)$$

Where  $\sigma_{Pb} = 497.5 - 0.1096 \times T$  is the surface tension of pure Pb and  $\sigma_{Sn} = 5582.8 - 0.0834 \times T$  is correspondingly surface tension of pure Sn. The values  $X_{Pb}$  and  $X_{Sn}$  indicated the corresponding mass fractions. The temperature is provided as independent variable in Kelvins.

The equation, provided by Butler, derived based on equilibria between the bulk phase and surface monolayer becomes for Pb:Sn system [13] as follows:

$$\sigma_{m,i,j} = \sigma_{Pb} + \frac{RT}{A_{Pb}} \ln \frac{1 - X_{Sn}^S}{1 - X_{Sn}^B} + \frac{1}{A_{Pb}} [G_{Pb}^S(T, X_{Sn}^S) - G_{Pb}^B(T, X_{Sn}^B)] \quad (1a)$$

or

$$\sigma_{m,i,j} = \sigma_{Sn} + \frac{RT}{A_{Sn}} \ln \frac{X_{Sn}^S}{X_{Sn}^B} + \frac{1}{A_{Sn}} [G_{Sn}^S(T, X_{Sn}^S) - G_{Sn}^B(T, X_{Sn}^B)] \quad (1b)$$

Where R is the gas constant [J/(mol.K)]; T is the temperature in Kelvins;  $\sigma_{Pb}$  and  $\sigma_{Sn}$  are the corresponding surface tensions of pure Pb and Sn;  $A_{Pb}$  and  $A_{Sn}$  are the correspondingly for Pb and Sn the partial molar surface area of a monolayer of Pb or Sn. It can be obtained from  $A_i = LN^{1/3}V_i^3$ . Here N is the Avogadro's number,  $V_i$  is the molar volume of the corresponding component. The parameter L is assumed to be 1.091 for liquid metals with close packed structure. The parameters  $X_{Sn}^S$  and  $X_{Sn}^B$  are correspondingly the molar fractions of the component, Sn at the liquid surface and

the bulk. The partial Gibbs energy excess is correspondingly  $G_k^S$  and  $G_k^B$  for the surface and the bulk for the component  $k = \{Sn, Pb\}$ . The excess of Gibbs energy relation between the surface and the bulk, is provided by the following relation:  $G_{Sn}^S(T, X_{Sn}^S) = \varepsilon G_{Sn}^B(T, X_{Sn}^B)$ . The parameter  $\varepsilon$  is the ratio of coordination number of the surface to that of the bulk phase. It is assumed 0.83 for the liquid metals [13].

The surface tension, analyzed by the proposed technique, in the current paper, is obtained under non-equilibrium conditions. Therefore, the corresponding theory must be applied in order to improve the predictions. Reference [14], provides the following relation:

$$\sigma_{ij} = \sigma_{m,ij} - [S^A + C(\beta)](\tau - \tau_m) + \frac{4}{3}\beta\sigma_v K \left[ \frac{1}{\sqrt{\tau}} + \frac{1}{\sqrt{\tau_m}} \right] \quad (2)$$

Where  $S_i^A = \frac{2}{3} \frac{\beta\sigma_v K}{\tau^{2/3}} + C(\beta)$ ,  $C(\beta)$  is an unknown function,  $K = \frac{\tau_0 \exp A}{\sqrt{2\pi}RA}$  with constant of integration A,  $\tau$  is the average time the atom spends on surface,  $\tau_0$  period of vibration for a surface atom;  $M$  is the molecular weight;  $R$  is the gas constant. The parameter  $\beta = \frac{\theta - \theta_e}{\theta_e}$  represents surface adsorption, based on Langmuir model. The parameter  $\theta$  is the fraction of the occupied sites, while the equilibrium fraction is  $\theta_e = \frac{Z\tau Ns}{1+Z\tau Ns}$ ;  $s$  is the occupied area per site,  $-1 \leq \beta \leq 0$ . The evaporation rate is:  $Z = \frac{P_v}{\sqrt{2\pi MRT}}$  and vapor pressure:  $P_v = \exp\left(A - \frac{\sigma_v}{RT}\right)$ . At equilibrium  $C(\beta)$  and  $\beta$  become zero and the equation is reduced to surface tension at constant equilibrium entropy.

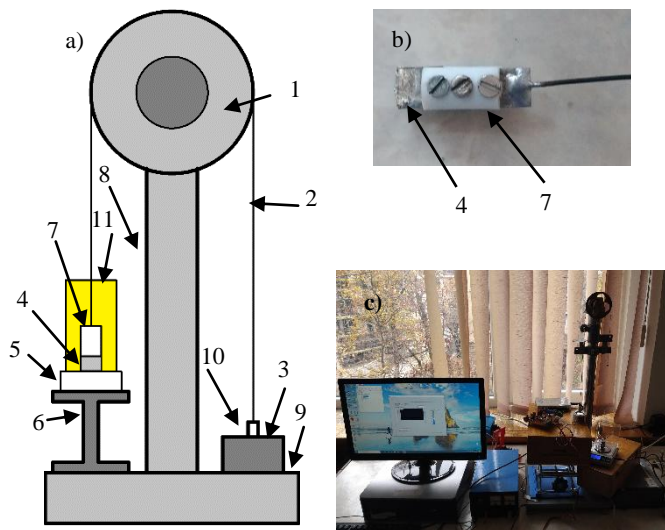


**Fig. 1** Experimental setup: a) schematic presentation of the measuring unit: 1-pulley, 2-non-expanding string, 3-balance scale, 4-Wilhelmy plate, 5-oven, 6- Z-axis movable table, 7-Wilhelmy plate holder, 8, 9-support of the system, 10-weight, 11- isolating container; b) picture of Wilhelmy plate with the holder; c) picture of the entire setup including the controllers and the computer.

### 3. Experimental setup

The experimental setup was designed in order to use the Wilhelmy plate method [15], a method that has relatively good stability. If the plate is properly prepared, the contact angle between the plate and the surface menisci is zero and therefore correction coefficients are not required for the measurement [15].

Schematic of the experimental setup is shown in Fig. 1a. We use an antivibration table 9, with pillar, 8, and a pulley, 1, on the top. Heating bed 5, is placed a top of a Z-axis movable supporting table 6. The tray is thermally isolated from the environment by a holder made of PTFE. We use HA2-60A or KERN 240-KB-3N balance scale, 3, that measure the calibration weight 10, with the mass of 50 g. The weight is connected by non-elastic cable 2, which

is a combination of stainless-steel chain and a flexible wire made by material with low heat transfer coefficient. The measurements of surface tension are performed by a traditional Wilhelmy plate with 10 mm length of the contact line. The plate, 4, is made of nickel with thickness of 300  $\mu\text{m}$ . The plate is then attached to a holder 7, made by PTFE, that insulate the plate from the wire, keeping it temperature constant. In order to achieve zero degree contact angle, before each measurement, the plate was cleaned and coated by a layer of solder (Fig. 5b). The other side of the holder is connected by stainless steel wire with diameter  $\varnothing 100 \mu\text{m}$  of length 100 mm, joined with the cable 2. The measuring unit is isolated by a glass container 11. This particular design, allows us, to separate thermally the plate, from the other part of the setup and keep the plate and the liquid metal, at the same temperature, with a minimal surface temperature gradient. In Fig. 1c is shown a picture of the experimental setup.

### 4. Materials and methods

Currently, the designed experimental setup is used for analysis the surface tension of three soldering alloys. The melting temperature ranges are presented in Table 1. The selected alloys in our study, are the following: Pb:Sn in ratio 40:60 is near to the eutectic point (Sn: 61.9 %). The other alloy has Pb:Sn content ratio 60:40. In addition, the surface tension of pure Sn melt is also considered to measurement. According to the specification, here Sn is 99.9%.

**Table 1:** Summary of the sample compositions [16].

Case		Melt. Temp., K Solidus	Melt. Temp., K Liquidus	Temp. K, Uses
A	Pb:Sn 40:60	456(183°C)	461(188°C)	(248°C)
B	Pb:Sn 60:40	456(183°C)	508(235°C)	(295°C)
C	Sn	505(232°C)	505(232°C)	(292°C)

Our intention is to investigate the surface tension of melt at relatively low temperatures, above the alloys melting ranges, under atmospheric pressure. At these conditions, the surface oxidation is not very intense, comparatively to the higher temperatures. In addition, at the selected temperature range, no significant structural transformations are expected. According to the available information, Sn oxidation is a threshold process that is initiated above the oxygen pressure of  $(3.0-6.2) \times 10^{-10}$  bars, [17], (the partial pressure of oxygen in Earth atmosphere is  $\sim 0.2$  bars). The oxidation of Sn exhibits a strong temperature dependence, [18]. A stable oxide layer of SnO is formed for less than 10 min above 673K (400°C), while below this point the process of oxidation is slower and it takes up to 60 min to reach a stable layer [18]. With increasing of the temperature, there coexists SnO and SnO<sub>2</sub>, until temperature of 923 K(650°C) is reached, where all SnO is converted to SnO<sub>2</sub> [19].

The oxidation of Pb is well studied. The process of PbO formation in a melt is a nucleation process. Below 753K (490 °C), the oxides of Pb exist in tetragonal form [20]. The created PbO crystals can aggregate and to form larger crystals [21].

The measurement procedure involves the following steps: Initially the sample is heated up to 573 K(300 C) with dipped measuring plate to heat sufficiently the entire system. After that the temperature is reduced to the desired value. The liquid surface is brushed off the formed oxides by a silicone brush before every single measurement. The measurements begin after the system isolation with the glass container. The process of measurement starts from the lowest desired temperature and continues in direction toward the temperature increasing. Each measurement under stabilized conditions is repeated at least three times after brushing off the surface. In order to estimate the degree of non-equilibrium, at the beginning of our investigation, we measured the temperature of air near the liquid surface. We found a stable temperature gradient of about 10 K.

The solidification of the analyzed specimens, after completion of our set of measurements, is recorded by HDMI digital camera-microscope with 3MP image sensor, resolution 102×1080, 1080P with video recording speed 30fps. Its magnification range, by the design, is 10x-220x.

## 5. Results and discussion

We performed measurement of the three alloys with declared compositions in paragraph 4. The observed results, presented in Fig. 2, are quite interesting: Two cases provide very stable systematic results: Pb:Sn in composition 40:60 and 60:40 (case A&B, Table 1). The surface kinetics of Sn oxidation of the pure Sn liquid substance did not allow proper measurements of surface tension with the current configuration of our setup (case C, Table 1).

The results from our measurements showed that the surface tension of Pb:Sn in ratio 40:60 is increased to values predicted by Eq. (1) for pure Sn (compared to the data without oxidation, Fig. 1), possibly because of formation of SnO. With increasing of the temperature, the surface tension gradient is low. This result is possibly because the oxidized Sn already dominates at the surface.

In the case with Pb:Sn ratio of 60:40, a formation PbO possibly dominates at the surface, because at temperatures below 240°C, Pb partially separates. During the solidification, Pb is in excess (case B, Table 1). On the surface it possibly reacts with atmospheric oxygen and because of nucleation, formation of growing aggregates can take place. In this case the surface tension is lowered to the measured surface tension of pure Pb. A higher gradient with the increasing of temperature is exhibit (comparing to the surface tension at non-oxidizing conditions).

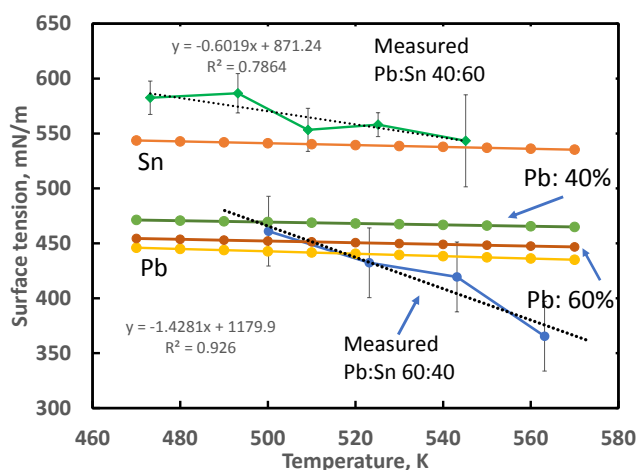


Fig. 2 Surface tension of Pb:Sn.

The performed experimental work allows to be analyzed the non-equilibrium contribution to surface tension that comes from the liquid surface oxidation. Based on the data, provided in Fig. 2 and combination of Eq. (2ab) with Eq. (3), we can write [22]:

$$\Delta\sigma_{i,j} = \sigma_{i,j} - \sigma_{m,i,j} \quad (4)$$

Where  $\sigma_{i,j}$  is the obtained theoretically surface tension from Eq. (1) and  $\sigma_{m,i,j}$  is the measured value. Based on this we estimate empirically the difference for Pb:Sn in ratio 40:60:

$$\Delta\sigma_{40:60} = 0.5249T - 380.68 \quad (5a)$$

Correspondingly, for ratio Pb:Sn 60:40 is obtained:

$$\Delta\sigma_{60:40} = 0.0134T + 10.567 \quad (5b)$$

In Eq. (5a) is shown that the adding surface energy rate because of oxidation and non-equilibrium thermal conditions is much higher in comparison to data in Eq. (5b). From the equations above is seen that the mixture near the eutectic point (of Pb:Sn in 40:60) stabilizes the surface tension as the added surface energy rate with increasing of the temperature is very low. However, the measurements of pure

Sn (Table 1, C) surface tension indicated that the first several minutes of Sn exposure on air, oxidation very actively takes place. This is indicated visually by the changing of the color of surface to yellow. Then, the formed oxide layer further stabilizes the surface properties of the liquid melt and suppresses the further oxidizing of Pb:Sn in ratio 40:60, contrary to the case 60:40, where is observed stronger gradient of the surface tension decrease with the increasing of the temperatures.

In order to understand better the processes, we recorded images of the solidification process and presented them below. This is helpful in providing a simple explanation of the obtained results. The pictures in Figs 3-5 represent the solid alloys shortly after the solidification of the investigated alloys, at the end of surface tension measurement. The cooling was performed by turning off the heating element and waiting the cooling of the samples to the ambient temperatures, 293 K, (natural speed). We selected this approach to cool the samples after several tests with controlled reduction of the speed of cooling below the natural but no differences were observed at the records of the surface solidification.

Figure 3 shows a picture of 60 % Sn and 40 % Pb sample surface shortly after its solidification. The formed structure consists from two constituent distinct phases: dark phase and crystalized structure [23] [24]. The dark occupied relatively large zones consist possibly from oxidized Pb, which remains on the surface. This conclusion is based on the fact that after solidification of Sn (Fig. 5) such dark phase formation is not observed.

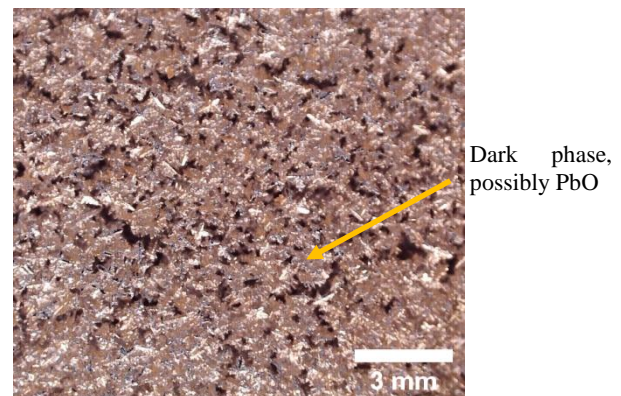


Fig. 3 Solidified melt Pb:Sn in ratio40:60 (POK60).

Figure 4 represents the surface of cooled and solidified sample of 40% Sn and 60% Pb near the melting point. It consists from two solid phases. However, the mixture is formed in a very small scale, and the phases are not distinguished on the picture. In our opinion, oxidized Pb is dominating over the surface.

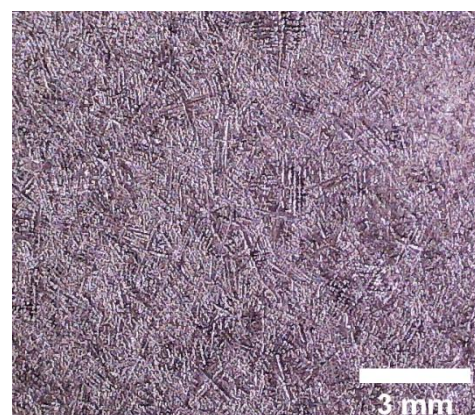


Fig. 4 Solidified melt Pb:Sn in ratio 60:40 ((POK40).

A picture of the solidified Sn is presented in Fig. 5. The structure looks very much lamellar. The surface color of the structure is nearly yellow at the solidification, which certainly indicates that a thin layer of SnO is covering the surface upon the oxidation.

For several minutes after exposure on air, just above the melting point, the surface obtains this specific yellow color. At the temperatures above 573 K, the color is changed to blue. This surface color changing is attributed to the transformation of SnO to SnO<sub>2</sub> at higher temperatures.

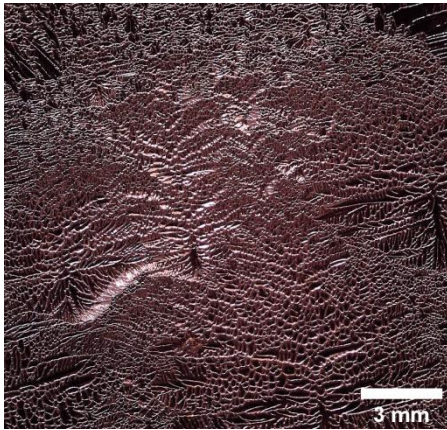


Fig. 5 Solidified Sn melt.

## 6. Conclusions

Based on the performed studies of the surface tension, we conclude that the proposed method of Wilhelmy plate is suitable for measurement of liquid metal surfaces even under non-equilibrium conditions. It is sensitive enough to be revealed the oxidation surface properties. We detected strong surface kinetics in Pb oxidation and the presence of oxidized Sn on the surface have the opposite stabilization effect.

The presence of PbO on the surface is acting toward reduction of surface tension in comparison with non-oxidized melt, while Sn oxides modify the surface tension in opposite direction, in comparison to the non-oxidized alloys. The significant Pb oxidation decrease the surface tension to become nearly the same as the surface tension of the pure Pb. The surface tension of the mixture Pb:Sn 40:60 became nearly at the same range as the pure Sn (See Fig. 2). The stabilization effects of oxidized Sn on the surface tension should be investigated in future.

## 7. References

1. L. L. Bircumshaw, *Phil. Mag*, **17**, 110, 181-191, (1934).
1. D. W. G. White, *Metall. Trans. B*, **2**, 3067–3071, (1971).
2. M. Kucharski M, *Arch. HUTN.*, **2**, 22, 181-194, (1977).
3. K. Nogi, K. Oishi and K. Ogino, *Mat. Trans., JIM*, **20**, 2, 137-145, (1989).
4. W. Gasior, Z. Moser and J. Pstrus, *J Phase Equilibria*, **25**, 1, 20-25, (2001).
5. I. Kaban, S. Mhiaoui, W. Hoyer and J.-G. Gasser, *J. Phys.: Condens. Matter*, **17**, 7867–7873, (2005).
6. E. A. Brandes and G. B. Brook, *Smithells Metal Reference*, 7-th ed., Oxford: Butterworth–Heinmann, (1998).
7. Y. Xi, L.-J. Liu and Z.-H. Chen, *Kovove Mater.*, **43**, 432-439, (2005).
8. Y. Kirshon, S. B. Shalom, M. Emuna, Y. Greenberg, J. Lee, G. Makov and E. Yahel, *MDPI materials*, **12**, 3999, (2019).
9. E. P. Loewen and A. T. Tokuhiko, *J. of Nucl. Sci. and Technol*, **40**, 8, 614–627, (2003).
10. J. R. Weeks, *Nucl. Eng. Des.*, **15**, 363-72, (1971).
11. W. G. Gale and T. C. Totemeier, Eds., *Soldering and Brasing, in Smithells Metals Reference Book*, 8-th ed., Academic Press, 34-1-34-22, (2004),
12. J. A. V. Butler, *Proc. Math. Phys. Eng. Sci.*, 348-375, (1932).
13. C. Maze and G. Burnet, *Surf. Sci.*, **7**, 411-418, (1977).
14. W. Contributors, *Wilhelmy plate*, Wikipedia, The Free Encyclopedia, 19 December 2020. [Online]. Available: [https://en.wikipedia.org/w/index.php?title=Wilhelmy\\_plate&oldid=989575010](https://en.wikipedia.org/w/index.php?title=Wilhelmy_plate&oldid=989575010). (Accessed 2 February 2021).
15. An Avnet Company, <https://www.farnell.com>, 2019. [Online]. Available: <http://www.farnell.com/datasheets/315929.pdf>. (Accessed 23 Jan. 2021).
16. A. Grigoriev, O. Shpurko, C. Steimer, P. S. Pershan, B. Ocko, M. Deutsch, L. Binhua, M. Meron, T. Graber and J. Gebhardt, *Surf. Sci.*, **575**, 3, 225-232, (2005).
17. E. Barreira, L. Pedrini, M. Boratto and L. Scalvi, *Intl. J. of Modern Phys. B*, **34**, 2050184-13p, (2020).
18. J. Geurfs, S. Rau, W. Richter and F. J. Schmitt, *Thin Solid Films*, **121**, 3, 217-225, (1984).
19. T. E. Weyand, *The oxidation kinetics of liquid lead and lead alloys*, University of Missouri–Rolla, (1970).
20. K. Gladinez, K. Rosseel, J. Lim., A. Marino, G. Heynderickx and A. Aerts, *Phys. Chem. Chem. Phys.*, **19**, 27593-27602, (2017).
21. Y.-B. K. Kang, *Calphad*, **50**, 23-31, (2015).
22. C. Basaran and R. Chandaroy, *Appl. Math. Model.*, **22**, 601-627, (1998).
23. P. T. Vianco, S. N. Burchett, M. K. Neilsen, D. A. Rejent and D. R. Frear, *J. Elec. Mater.*, **28**, 1290-1298, (1999).